



Association Between Circulating CD4⁺ T Cell Methylation Signatures of Network-Oriented SOCS3 Gene and Hemodynamics in Patients Suffering Pulmonary Arterial Hypertension

Giuditta Benincasa¹ · Bradley A. Maron^{2,3} · Ornella Affinito⁴ · Michele D'Alto⁵ · Monica Franzese⁴ · Paola Argiento⁵ · Concetta Schiano¹ · Emanuele Romeo⁵ · Paola Bontempo⁶ · Paolo Golino⁵ · Liberato Berrino⁷ · Joseph Loscalzo² · Claudio Napoli^{1,4}

Received: 9 May 2022 / Accepted: 19 July 2022 / Published online: 12 August 2022
© The Author(s) 2022

Abstract

Pathogenic DNA methylation changes may be involved in pulmonary arterial hypertension (PAH) onset and its progression, but there is no data on potential associations with patient-derived hemodynamic parameters. The reduced representation bisulfite sequencing (RRBS) platform identified $N=631$ differentially methylated CpG sites which annotated to $N=408$ genes (DMGs) in circulating CD4⁺ T cells isolated from PAH patients vs. healthy controls (CTRLs). A promoter-restricted network analysis established the PAH subnetwork that included 5 hub DMGs (*SOCS3*, *GNAS*, *ITGAL*, *NCOR2*, *NFIC*) and 5 non-hub DMGs (*NR4A2*, *GRM2*, *PGK1*, *STMN1*, *LIMS2*). The functional analysis revealed that the *SOCS3* gene was the most recurrent among the top ten significant pathways enriching the PAH subnetwork, including the growth hormone receptor and the interleukin-6 signaling. Correlation analysis showed that the promoter methylation levels of each network-oriented DMG were associated individually with hemodynamic parameters. In particular, *SOCS3* hypomethylation was negatively associated with right atrial pressure (RAP) and positively associated with cardiac index (CI) ($|r| \geq 0.6$). A significant upregulation of the *SOCS3*, *ITGAL*, *NFIC*, *NCOR2*, and *PGK1* mRNA levels (qRT-PCR) in peripheral blood mononuclear cells from PAH patients vs. CTRLs was found ($P \leq 0.05$). By immunoblotting, a significant upregulation of the SOCS3 protein was confirmed in PAH patients vs. CTRLs ($P < 0.01$). This is the first network-oriented study which integrates circulating CD4⁺ T cell DNA methylation signatures, hemodynamic parameters, and validation experiments in PAH patients at first diagnosis or early follow-up. Our data suggests that *SOCS3* gene might be involved in PAH pathogenesis and serve as potential prognostic biomarker.

Keywords Pulmonary Arterial Hypertension · DNA Methylation · CD4⁺ T cells · Network Analysis · Hemodynamic Parameters

Associate Editor Paul J. R. Barton oversaw the review of this article

Giuditta Benincasa, Bradley A. Maron, and Ornella Affinito contributed equally to this work.

✉ Giuditta Benincasa
giuditta.benincasa@unicampania.it

¹ Department of Advanced Medical and Surgical Sciences (DAMSS), University of Campania “Luigi Vanvitelli”, 80138 Naples, Italy

² Division of Cardiovascular Medicine, Department of Medicine, Brigham and Women’s Hospital, MB, Boston, USA

³ Harvard Medical School, Boston, MA, USA

Abbreviations

BSG	Basigin
CGIs	CpG islands
CI	Cardiac index
CLEC4G	C-type lectin domain family 4 member G

⁴ IRCCS SDN, Naples, Italy

⁵ Department of Cardiology, Monaldi Hospital, University of Campania “Luigi Vanvitelli”, Naples, Italy

⁶ Department of Precision Medicine, University of Campania “Luigi Vanvitelli”, Naples, Italy

⁷ Department of Experimental Medicine, University of Campania “Luigi Vanvitelli”, Naples, Italy

CTBP2	C-terminal binding protein 2
DLC1	DLC1 Rho Gtpase activating protein
dmCpGs	Differentially methylated CpG sites
DMGs	Differentially methylated genes
DNMT3B	DNA methyltransferase 3 beta
DPPA4	Developmental pluripotency associated 4
gDNA	Genomic DNA
GNAS	Guanine nucleotide binding protein (G protein), alpha stimulating activity
GRM2	Glutamate metabotropic receptor 2
IL	Interleukin
ITGAL	Integrin subunit alpha L
LAMA5	Laminin subunit alpha 5
LIMS2	LIM zinc finger domain containing 2
mPAP	Mean pulmonary arterial pressure
NCOR2	Nuclear receptor corepressor 2
NFIC	Nuclear factor I C
NR4A2	Nuclear receptor subfamily 4 group A member 2
PAH	Pulmonary arterial hypertension
PCWP	Pulmonary capillary wedge pressure
PBMCs	Peripheral blood mononuclear cells
PGK1	Phosphoglycerate kinase 1
PKP1	Plakophilin 1
PPIs	Protein-protein interactions
PVR	Pulmonary vascular pressure
qRT-PCR	Quantitative real-time PCR assay
RAP	Right atrial pressure
RHC	Right heart catheterization
RNF166	Ring finger protein 166
RPTOR	Regulatory associated protein of MTOR complex 1
RRBS	Reduced representation bisulfite sequencing
SF3A1	Splicing factor 3a subunit 1
SH3BP4	SH3 domain binding protein 4
SOCS3	Suppressor of cytokine signaling 3
STAT3	Signal transducer and activator of transcription 3
STMN1	Stathmin 1
TSS	Transcription start site
UTRs	Untranslated regions

Introduction

Pulmonary arterial hypertension (PAH) is a highly morbid cardiopulmonary disease associated with decreased lifespan despite the availability of vasodilator and other therapies [1–4]. In clinical trials and in practice, treatment response is variable across different PAH subgroups and individual patients [1–4]. This is ascribed to a high heterogeneity in the molecular basis of vascular and cardiac

remodeling that underlies PAH, for which no specific biomarkers are established yet [1–4]. The complex nature of PAH suggests that epigenetic-sensitive mechanisms, mainly guided by DNA methylation, are key players underlying a progressive pulmonary vascular remodeling which leads to increased vascular resistance and a concomitant right ventricle remodeling [1]. DNA methylation is a covalent enzymatic modification mediated by DNA methyltransferase which add one or more methyl groups at the 5'-carbon of cytosine bases localized in 5'-CpG-3' dinucleotides [5]. These latter motifs are most abundant in CpG island (CGI) regions annotated to promoters which can regulate the rate of gene expression at transcriptional level. Generally, there is an inverse relationship between the grade of DNA methylation into the CGI-promoter regions and gene activity, for which DNA hypermethylation is prone to silence gene expression, whereas DNA hypomethylation is transcriptionally more permissive [5]. Previous clinical evidence showed that alterations in DNA methylation signatures were linked to lipid metabolism, incomplete penetrance, and pro-inflammatory pathways [1, 6] which were strongly implicated in the PAH pathogenesis [7, 8]. However, no previous study investigated DNA methylation changes and their potential associations with hemodynamic parameters in PAH patients.

Thus, we leveraged the large CLEOPAHTRA trial (NCT04282434 at clinicaltrials.gov) of well-phenotypes patients to test the hypothesis that PAH patients are distinct from healthy controls by virtue of circulating CD4⁺ T cell DNA methylation signatures, which, in turn, may be relevant for phenotyping and prognostication of affected patients. The goal of our study was to apply a network analysis to patient-derived CD4⁺ T cell methylation profiles to discover novel potential pathogenic mechanisms in patients with PAH at time of diagnosis or early follow-up. Despite the well-known role of monocytes and myeloid cells in PAH response [7], CD4⁺ T cells have been understudied and are now emerging as key players in pulmonary vascular remodeling both in experimental [9–12] and clinical studies [13–16]. Furthermore, based on our previous experience [17, 18], we choose circulating CD4⁺ T cells because of their utility in capturing DNA methylation signatures and molecular pathways mirroring a potential clinical significance.

Here, we perform a novel research program integrating clinical epigenetics and network medicine analytic approaches to advance precision medicine in PAH. Findings from this study have direct translational potential ranging from biomarker discovery and validation to therapeutic target identification that can be studied further in future investigations.

Material and Methods

Ethics Statement

This study was approved by the Local Ethics Committee at University of Campania “L. Vanvitelli” Naples, Italy (N. protocol 800/2019). All individuals in the study provided written informed consent for the collection of samples and subsequent analysis. This study was conducted according to the principles and guidelines expressed in the Declaration of Helsinki.

Study Population

Between April 2019 and January 2020, we enrolled in the CLEOPAHTRA trial (NCT04282434) a total of $N=25$ consecutive patients with Pulmonary Hypertension (PAH) WHO Groups I who were diagnosed by right heart catheterization (RHC) at the Pulmonary Hypertension Centre of Monaldi Hospital, University of Campania “L. Vanvitelli” (Naples, Italy), according to diagnostic criteria at that time [19]. Specifically, PAH was diagnosed by mean pulmonary arterial pressure (mPAP) ≥ 25 mmHg at rest or mPAP ≥ 30 mmHg with exercise, pulmonary capillary wedge pressure (PCWP) ≤ 15 mmHg, and pulmonary vascular resistance (PVR) ≥ 240 dynes-sec-cm-5 (e.g., ≥ 3.0 wood units). Patients were grouped in idiopathic PAH (IPAH, $N=13$), PAH associated with congenital heart disease (PAH-CHD, $N=5$), PAH associated with systemic sclerosis (PAH-SSc, $N=5$), and PAH associated with portal hypertension (POPH, $N=2$). PAH patients were stratified using a simplified risk assessment tool that quantifies the number of low-risk criteria (NYHA/WHO: I–II, 6MWD > 440 m, RAP < 8 mmHg, CI > 2.5 L/min/m²). Patients with low (3–4 parameters), intermediate (2 parameters), and high (1–0 parameters) risk features have an estimated 1-year risk of death of $< 5\%$, 5–10%, and $> 10\%$, respectively. Patients who meet the criteria for inclusion into PH WHO Groups II, III, IV, or V were excluded from the study. To avoid confounder effects, patients with known history of cancer, active infections, and chronic or immune-mediated diseases were not enrolled. A total of $N=16$ volunteer blood donors served as healthy controls (CTRLs) and were recruited from the U.O.C. Divisione di Immunologia Clinica, Immunoematologia, Medicina Trasfusionale e Immunologia dei Trapianti, Dipartimento di Medicina Interna e Specialistica, AOU “L. Vanvitelli” University of Campania (Naples, Italy). Clinical characteristics of PAH patients are summarized in Supplementary Table 1.

Flowchart for Discovery and Validation of DNA Methylation Signatures

As previously described [17, 18], we harvested approximately 10–15 mL of peripheral blood from the jugular vein of $N=25$ PAH patients during RHC and the antecubital vein of $N=16$ CTRLs during blood donation. Within 2 h, we collected peripheral blood mononuclear cells (PBMCs),

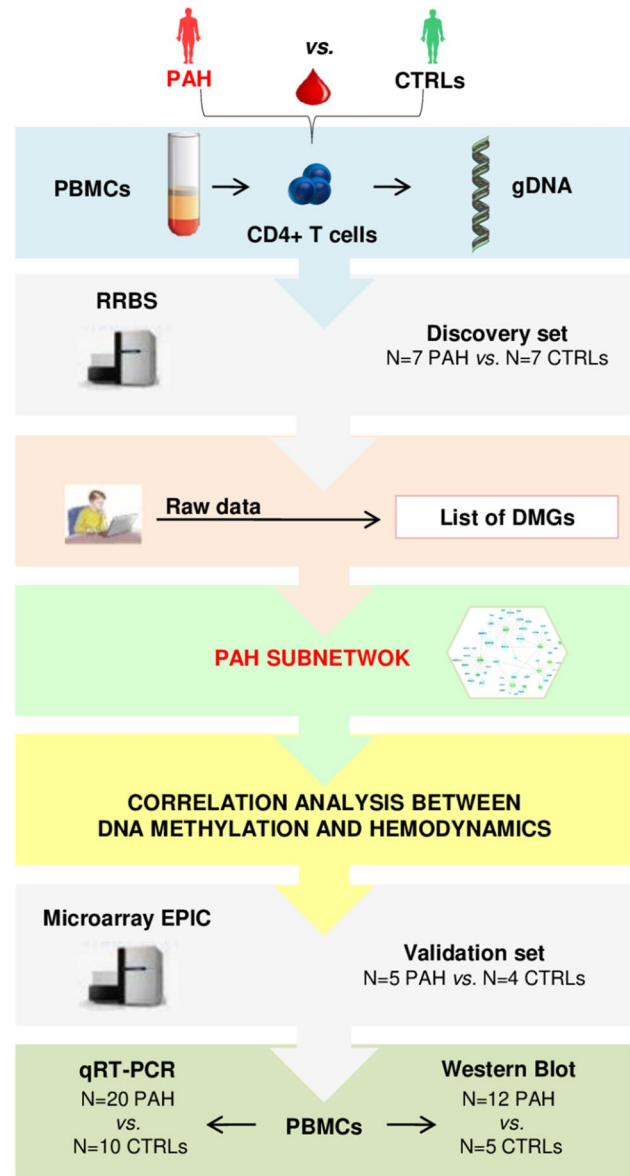


Fig. 1 Study design. This flowchart shows the network-oriented strategy used to build the PAH subnetwork via integrating circulating CD4⁺ T cell DNA methylation signatures and hemodynamic parameters. Abbreviations: CTRLs, controls; DMGs, differentially methylated genes; gDNA, genomic DNA; PAH, pulmonary arterial hypertension; PBMCs, peripheral blood mononuclear cells; RRBS, reduced representation bisulfite sequencing

isolated CD4⁺ T cells, and extracted genomic DNA (gDNA). Based on PBMC recovery, we also stored some cellular aliquots for successive validation experiments (Data Supplement).

The flowchart for discovery and validation of DNA methylation signatures is shown in the Fig. 1. As a discovery set, $N=7$ PAH patients vs. $N=7$ CTRLs were selected for reduced representation bisulfite sequencing (RRBS), which was performed at the Genomix4Life S.r.l. (Salerno, Italy) (<https://www.genomix4life.com/it/>). To profile genome-wide DNA methylation signatures in the discovery set, we selected the subset of gDNA samples which was of highest quality and highest yield (≥ 2.5 – 3.0 μg). Then, raw data were analyzed via network analysis to obtain the PAH subnetwork (or PAH interactome) which was successively validated in an independent set of $N=5$ PAH patients vs. $N=4$ CTRLs. For validation of network-oriented DNA methylation signatures, we chose the Infinium Human Methylation EPIC BeadChip platform which was performed at the DKFZ Genomics and Proteomics Core Facility (GPCF) in Heidelberg (Germany) (https://dtk.dkfz.de/en/sites/heidelberg/core_facilities) (Data Supplement). Successively, the functional effects of DNA methylation changes were validated in PBMCs using traditional molecular biology techniques, such as qRT-PCR and Western blotting.

DNA Sequence Processing and Alignment

RRBS raw reads were assessed for quality using FastQC (v011.8, Babraham Bioinformatics, UK) and trimmed using TrimGalore (v0.6.3, Babraham Bioinformatics, UK). Cytosine methylation calls was performed using the Bismark methylation extractor (Supplementary Table 2). Data from Infinium Human Methylation EPIC BeadChip processing were quantile-normalized using the function `normalize.quantiles` from the Bioconductor package “`preprocessCore`” (Data Supplement). Raw data have been deposited in the NCBI Gene Expression Omnibus (GEO) database under the accession number GSE165360 (<https://www.ncbi.nlm.nih.gov/geo/query/acc.cgi?acc=GSE165360>).

qRT-PCR

TRIzol solution (Thermo Fischer Scientific, USA) was used to extract total RNA from frozen PBMCs of $N=20$ PAH vs. $N=10$ CTRLs according to the manufacturer’s instructions. Oligonucleotide sequences are reported in the Supplementary Table 3. The relative mRNA expression levels were measured using the CFX96 touch real-time PCR detection system (BioRad Laboratories, Ltd, USA) (Data Supplement). Expression values were analyzed with the delta Ct (ΔCt) method using the equation $\Delta\text{Ct} = \text{Ct}_{\text{reference}} - \text{Ct}_{\text{target}}$. The ΔCt values of the

target genes were normalized to that of the housekeeping gene encoding RPS18 [20]. Each sample was analyzed in duplicate, and relative expression data are given as Fold Change (FC, $2^{-\Delta\Delta\text{Ct}}$).

Western Blot

Western blot analysis was performed using frozen PBMCs from $N=12$ PAH patients vs. $N=5$ CTRLs. The membranes were incubated with both mouse anti-human anti-SOCS3 (OriGene, #TA502991) at a dilution 1:1000 and mouse anti-human anti-GAPDH at a dilution 1:5000 (Santa-Cruz #sc-365062) overnight at 4 °C and next incubated with peroxidase-labeled secondary antibody and visualized using the ECL detection system (Data Supplement). GAPDH protein served as loading control and was detected on the same membranes for normalizing the signals.

Bioinformatic Analysis and Data Visualization

CpG Differential Methylation Analysis

We identified differentially methylated CpGs (dmCpGs) and annotated genes by comparing the CpG site methylation status in patients with PAH vs. CTRLs using the R package `methyKit` (v1.10.0) [21], after removing any potential batch effects. Coverage values between samples were normalized by default, and read coverage per base (Supplementary Figs. 1 and 2) was calculated. We then defined as dmCpGs those CpG sites with more than 20% methylation differences (ΔMI) and q value < 0.05 , after applying logistic regression using the SLIM method to correct the p value for multiple hypothesis testing.

Annotation of Differentially Methylated CpG Sites (dmCpGs)

The R package `ChIPseeker` (v1.20.0) [22] provided detailed annotation about the percentage of dmCpGs in PAH vs. CTRLs, which was located in promoters, coding sequences, introns, distal intergenic regions, and 5’ and 3’ untranslated regions (UTRs). Next, annotation of CGIs and CpG shores was obtained from the UCSC website (<http://genome.ucsc.edu/>; hg38). For clarity, we defined genes annotated to dmCpGs as differentially methylated genes (DMGs).

Network Analysis

Lung-Specific DNA Methylation-PPI Subnetworks

We used the NetworkAnalyst 3.0 tool (<http://www.networkanalyst.ca>) [23] to build two unique DNA

methylation-protein-protein interaction (PPI) subnetworks in PAH. Irrespective from their genomic localization, we mapped separately $N=230$ hypermethylated and $N=178$ hypomethylated DMGs (defined as “seed genes”) into the lung-specific PPI network from the DifferentialNet database. In order to identify hub DMGs, we used the *centrality degree* as network topological measure. We defined hubs those DMGs having *centrality degree* ≥ 10 .

Promoter-Restricted PAH Subnetwork

We built a PPI network between DMGs annotated to promoters ($N=114$) and known PAH-related genes as per the DisGeNET database ($N=172$) [24] by using Cytoscape v.3.7.2 [25] and the associated application ReactomeFIViz [26]. Briefly, we first downloaded the list of known PAH-related genes by searching the DisGeNET website using the following keywords: “idiopathic pulmonary arterial hypertension,” “pulmonary arterial hypertension associated with portal hypertension,” and “pulmonary arterial hypertension associated with connective tissue disease.” Each of the PAH-related genes was annotated with supporting publications. We removed genes that were annotated with only one publication to rule out potential false positives. Next, we constructed a PPI network linking DMGs and known PAH-related genes. In order to select hub DMGs with the strongest number of links to their known PAH-related interactors, we chose the *centrality degree* ≥ 10 and extracted a subnetwork for each of hub DMGs. Finally, each subnetwork was depicted using Cytoscape’s merge function [27].

Statistical Analysis

All analyses were performed using the R statistical package (version 3.6.2) (www.cran.r-project.org). The Shapiro–Wilk normality test was used to assess normality of data. The F test was used to evaluate the homogeneity of variance. Statistical significance was computed using two-tailed Student’s *T*-test if variables fulfilled the assumptions of a parametric test; otherwise, the Wilcoxon rank sum exact test was used. Correlation analysis (Pearson’s correlation or Spearman’s correlation) and linear regression were used to evaluate possible associations between hemodynamic parameters and DNA methylation. Statistical tests were considered significant if the *p* value ≤ 0.05 .

Power Analysis

For the sample size calculation, we considered the total number of annotated genes and the proportion of

non-DMGs. We used the R package “ssizeRNA” (version 1.3.1) which gives the power vs. sample size curve estimated by a simulation method using a negative binomial distribution. We determined the sample size with the following parameters: an achieved power of 0.8 at FDR = 0.05. We determined the sample size and assessed the power for detecting DMGs. This analysis revealed that our total sample size of $N=14$ patients for $N=408$ DMGs provided an estimated power of 0.74 at FDR = 0.05, given the dispersion of the data, as reported in the Supplementary Fig. 3.

Results

Clinical characteristics of PAH patients vs. CTRLs enrolled in the discovery set are described in Data Supplement and are summarized in Supplementary Table 4. Briefly, we identified 631 dmCpGs ($|\Delta M| \geq 20\%$, $q\text{-val} < 0.05$), of which 65% ($N=410$) were hypermethylated and 35% ($N=221$) were hypomethylated in PAH patients vs. CTRLs (Supplementary Fig. 4A). The majority of the dmCpGs were located within annotated distal intergenic regions (38.54% vs. 31.22% in hypermethylated and hypomethylated clusters, respectively) followed by promoters, defined as ± 1 kb to the transcription start site (TSS) (22.93% vs. 23.53% in hypermethylated and hypomethylated clusters, respectively) (Supplementary Fig. 4B–C). Manhattan plot showed that most dmCpGs were localized on chromosomes 20 (~11%) and 7 (~7%) (Supplementary Fig. 5A). When interrogating the distribution of the dmCpGs in the context of CGIs and CpG shores, most dmCpGs were found in CGIs associated with promoters ($N=116/251$, 46%) (Supplementary Fig. 5B). For brevity, the top 40 hypermethylated and hypomethylated dmCpGs are shown in Supplementary Tables 5 and 6, respectively. Our analysis showed $N=230$ hypermethylated and $N=178$ hypomethylated DMGs; rarely, DMGs showed both hypermethylation and hypomethylation in their genic regions (5 genes; 0.01%). The DMGs were classified with respect to gene type (Supplementary Fig. 5C–D) and ranked in descending order as: protein-coding genes > long non-coding genes > microRNAs > pseudogenes > unannotated nucleotides.

Global Network Analysis

The hypermethylated lung-specific DNA methylation-PPI subnetwork included 867 nodes, 996 edges, and

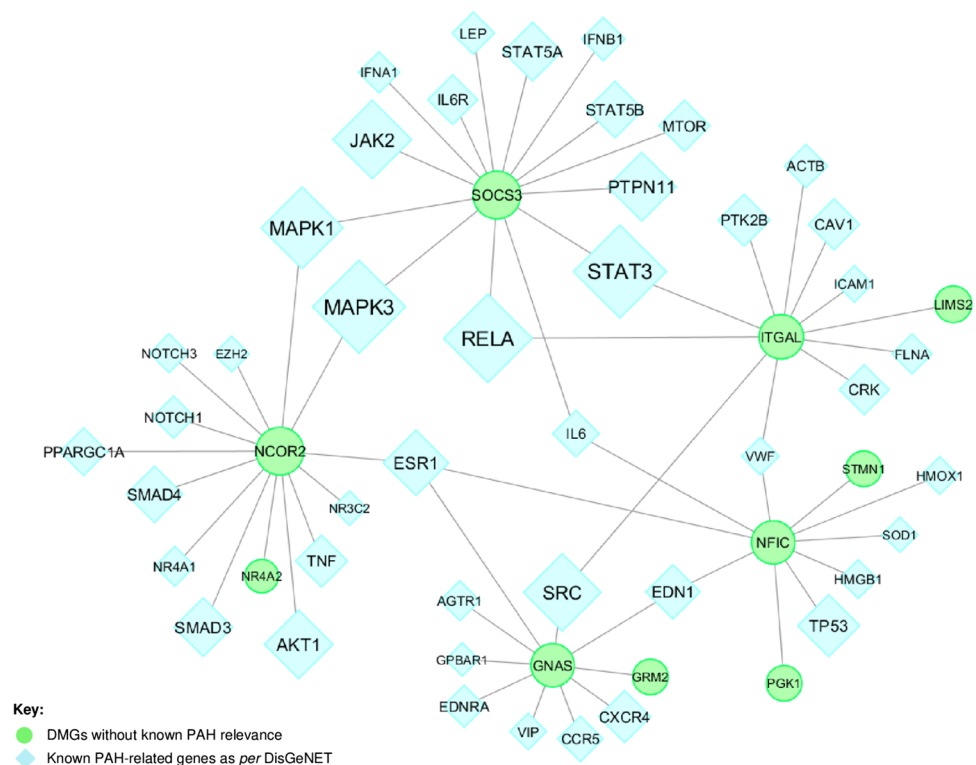
84 seeds (Supplementary Fig. 6). We identified $N = 28$ hub DMGs of which 32% ($N = 9/28$) was annotated to promoter regions (Supplementary Table 7). These included *RPTOR* [28], *CTBP2* [29], and *PGK1* [30] genes, which have been implicated previously in the pathogenesis of PAH. By contrast, *NCOR2*, *NR4A2*, *PKP1*, *DNMT3B*, *SH3BP4*, and *CLEC4G* genes were in the network but have not been reported previously as associated with PAH, thereby suggesting that these are novel epigenetic mediators of PAH. The hypomethylated lung-specific DNA methylation-PPI subnetwork retrieved 763 nodes, 882 edges, and 68 seeds (Supplementary Fig. 7). Among the hub DMGs ($N = 25$), the major percentage (36%, $N = 9/25$) was annotated to promoter regions (Supplementary Table 8). Previous evidence showed that *SOCS3* [31], *BSG* [32], *DLC1* [33], and *GNAS* [34] were potentially involved in PAH, whereas *DPPA4*, *LAMA5*, *SF3A1*, and *RNF166* had no previously recognized association. Globally, these results supported our successive promoter-restricted network analysis.

PAH Subnetwork

Building “PAH-specific subnetworks” represents a powerful bioinformatic strategy to identify novel potential

candidate genes and pathways involved in PAH pathogenesis [35, 36]. The core assumption of this analysis was that a DMG can interact with many known PAH-related genes and, therefore, may also be functionally relevant to the development of PAH. Our PAH subnetwork (Fig. 2) was characterized by 54 nodes and 59 edges in which PPIs linked 5 hub DMGs (*SOCS3*, *ITGAL*, *GNAS*, *NCOR2*, *NFIC*) to known PAH-related genes. In addition, 5 (non-hub) DMGs (*NR4A2*, *GRM2*, *PGK1*, *STMN1*, *LIMS2*) were linked to hubs (Supplementary Table 9). We suggest that these 10 network-oriented DMGs may affect or be affected themselves by the activities of their interacting partners with subsequent functional implications in the pathogenesis of PAH. Among the 10 network-oriented DMGs, none had PAH relevance as per DisGeNET; however, *PGK1* [30], *SOCS3* [31], and *GNAS* [34] genes were previously implicated in the pathogenesis of PAH or PAH drug responsiveness. The overrepresentation analysis (ORA) highlighted that the growth hormone receptor-, the interleukin-, and mainly the interleukin-6 (IL-6)- signaling were the most significant pathways of the PAH subnetwork (red circles) (Fig. 3). The inspection of genes enriching the top ten significant pathways (Supplementary Table 10) revealed that the *SOCS3* gene was the most recurrent than other network-oriented DMGs.

Fig. 2 The PAH subnetwork. The interactome shows 5 hub DMGs and 5 non-hub DMGs (green circles) linked through physical interactions (grey links) to specific known PAH-related genes as per DisGeNET (light blue diamonds). The size of both circles and diamonds is scaled according to the *centrality degree* and *betweenness centrality* measures. Original source: Cytoscape v.3.7.2 software



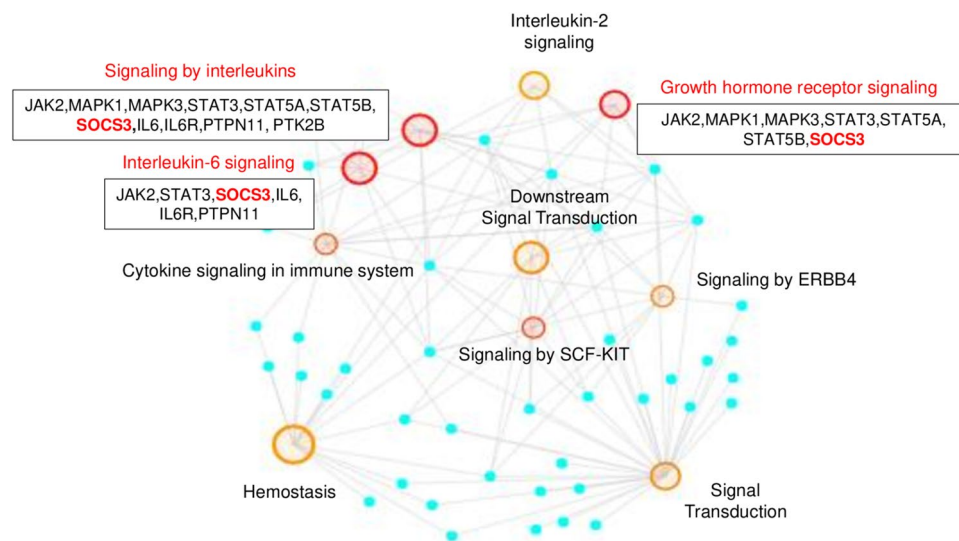


Fig. 3 Overrepresentation analysis (ORA). This figure shows the top ten significant pathways enriched by the genes of the PAH subnetwork through REACTOME database. Each pathway is indicated by a red or orange circle according to their p value (red circles correspond to the most significant p values). The circle size corresponds to the number of genes enriching that pathway. The small light blue circles represent the input gene list (54 nodes) and are located in the network periphery. ORA counts the number of genes shared by an input gene set and each annotated gene set, and applies a statistical test

(the cumulative hyper-geometric test) to calculate the statistical significance of the overlap. A p value cutoff ($p < 0.05$) is then applied to select the annotated gene sets that have statistically significant overlaps with the input gene set. The IL-6 signaling axis, the growth hormone receptor signaling, and the interleukin signaling (highlighted in red) reached the highest statistical significance. The network-oriented *SOCS3* gene was the most recurrent in the top significant pathways. Original source: NetworkAnalyst 3.0 software

Validation Set of Experiments

To assess the robustness of RRBS, we validated the methylation trends of our 10 network-oriented DMGs through two Infinium Human Methylation EPIC BeadChip arrays with the same content of probes in an independent set of $N = 5$ PAH patients and $N = 4$ CTRLs. Clinical characteristics of PAH patients are summarized in Supplementary Table 11. Starting with overlapping CpGs between the two arrays, we considered only those that confirmed the RRBS trend for each network-oriented DMG (Supplementary Table 12). We observed that hypermethylation of *NCOR2* and *NFIC* genes was confirmed in approximately 54% and 48% of detected CpGs, respectively, whereas analysis of *SOCS3*, *ITGAL*, and *GNAS* genes confirmed hypomethylation of approximately 69%, 79%, and 38% of detected CpGs, respectively. In addition, hypermethylation of *NR4A2*, *GRM2*, and *PGK1* genes was confirmed in approximately 64%, 65%, and 88% of detected CpGs, respectively, while hypomethylation of *STMN1* and *LIMS2* genes was confirmed in approximately 50% and 54% of detected CpGs, respectively. The CpG methylation distributions for the 10 network-oriented DMGs are shown in Supplementary Fig. 8.

Network-Oriented Promoter DNA Methylation Levels Associate with Patient-Level Hemodynamics

In Fig. 4A, the heatmap shows the methylation status (hypomethylation in red and hypermethylation in yellow) of significant dmCpGs ($N = 16$) which were annotated to network-oriented promoters discriminating CTRLs vs. PAH patients. However, each of them failed in discriminating IPAH vs. Associated-PAH patients. Correlation analysis was performed to evaluate whether promoter methylation levels were associated individually with hemodynamic parameters, including mPAP, PVR, right atrial pressure (RAP), and cardiac index (CI). We observed that each of these 10 network-oriented DMGs was strongly correlated ($|r| \geq 0.6$) with at least one of the four hemodynamic parameters both in IPAH (Fig. 4B) and Associated-PAH (Fig. 4C), even if a statistical significance was reached only for the *GNAS* gene. Besides, we observed that a panel of DMGs was negatively correlated (red signal) with RAP and positively correlated (blue signal) with CI (or vice versa), which are the most robust indicators of right ventricle function and prognosis. This occurred in 5/10 network-oriented DMGs (*SOCS3*, *ITGAL*, *GNAS*, *NR4A2*, and *GRM2*) in IPAH

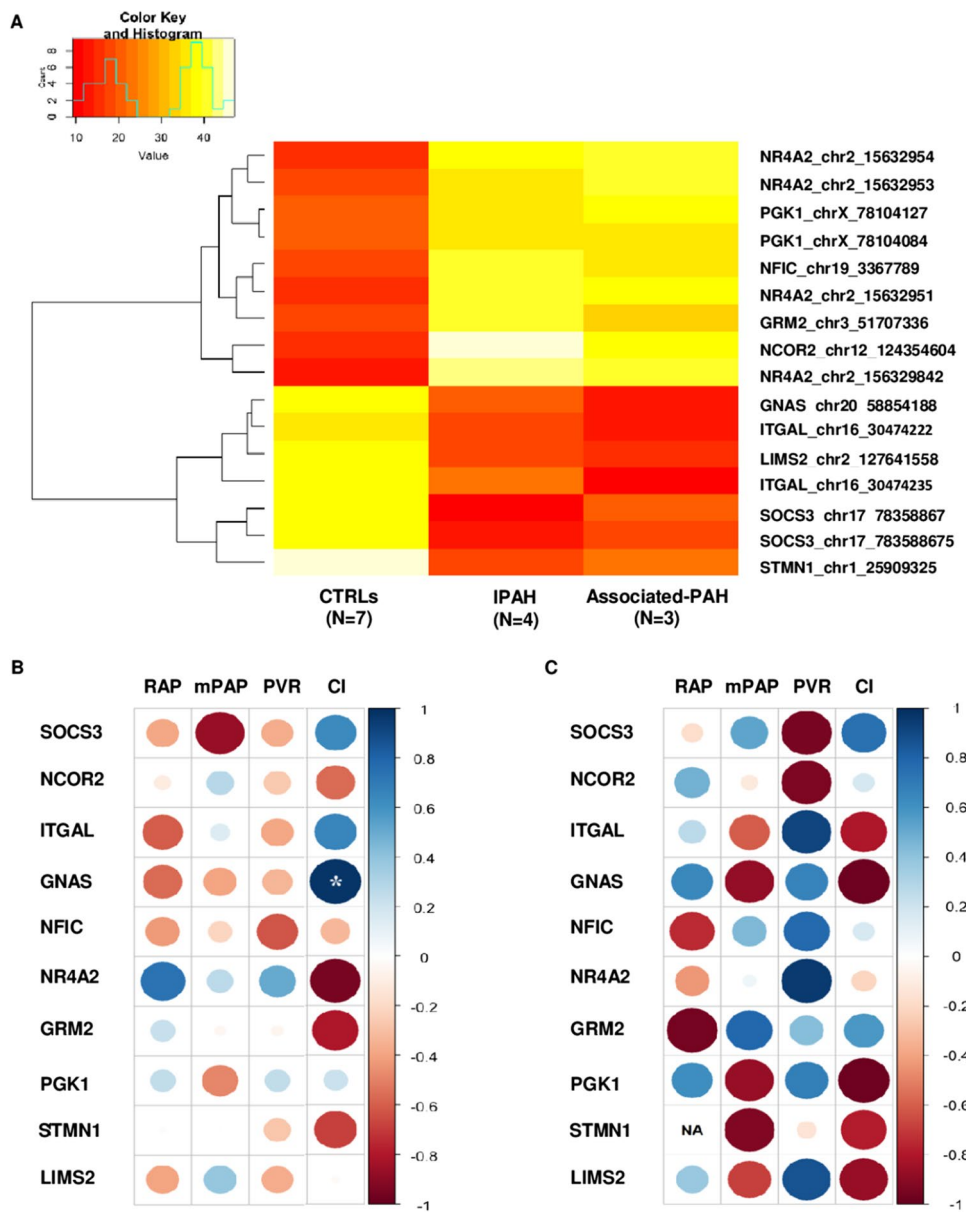


Fig. 4 Association between network-oriented promoter DNA methylation levels and hemodynamic parameters. **A** Unsupervised hierarchical clustering shows the mean methylation of the dmCpGs associated with the hub and non-hub DMGs. DNA methylation values of each dmCpG (rows) are averaged within the pre-classified group (column), including CTRLs ($N=7$) vs. IPAH ($N=4$) and Associated-PAH ($N=3$). The color key indicates DNA methylation status; red/orange represents hypomethylated DMGs and yellow/white represents hypermethylated DMGs. Correlograms show the Pearson's correlation between promoter DNA methylation levels of each network-oriented DMG and hemodynamic parameters in IPAH (**B**) or Associated-PAH (**C**). Circle size is scaled by the correlation coefficient. Blue and red

colors designate, respectively, positive and negative correlations. The asterisk (*) indicates significant correlations ($p \leq 0.05$). Abbreviations: PAH, pulmonary arterial hypertension; CI, cardiac index; ITGAL, integrin subunit alpha L; GNAS guanine nucleotide binding protein (G protein), alpha stimulating activity; GRM2, glutamate metabotropic receptor 2; LIMS2, LIM zinc finger domain containing 2; mPAP, mean pulmonary arterial pressure; NCOR2, nuclear receptor corepressor 2; NFIC, nuclear factor I C; NR4A2, nuclear receptor subfamily 4 group A member 2; PGK1, phosphoglycerate kinase 1; PVR, pulmonary vascular pressure; RAP, right atrial pressure; SOCS3, suppressor of cytokine signaling 3; STMN1, stathmin

(Fig. 4B) and 7/10 network-oriented DMGs in Associated-PAH (*SOCS3*, *ITGAL*, *GNAS*, *NFIC*, *GRM2*, *PGK1*, and *LIMS2*) (Fig. 4C). We also noted that *SOCS3* hypomethylation was negatively associated with RAP (red

signal) and positively associated with CI (blu signal) in both IPAH ($|r| = -0.4$ and $|r| = 0.6$, respectively) and Associated-PAH ($|r| = -0.2$ and $|r| = 0.7$, respectively) patients suggesting a potential prognostic biomarker.

Transcriptional Profiles of Network-Oriented *SOCS3*, *ITGAL*, *NFIC*, *NCOR2*, and *PGK1* DMGs Discriminate PAH Patients vs. CTRLs

Since promoter DNA methylation levels can affect gene expression at transcriptional level, we first determined if differences in mRNA levels of the 10 network-oriented DMGs were reliably detected in PBMCs by qRT-PCR. We chose PBMCs for two reasons: first, the recovery of CD4⁺ T cells from each peripheral blood biospecimen did not allow to extract also total mRNA; second, PBMCs represent a more easily accessible biospecimen than CD4⁺ T cells for potential clinical usefulness. For qRT-PCR experiments, we used PBMCs from $N=20$ PAH patients ($N=10$ Associated-PAH vs. 10 IPAH) vs. 10 CTRLs. In this experimental set, we included study participants from discovery set, validation set, as well as external subjects (Supplementary Table 13). Irrespective from promoter DNA methylation status, relative expression data (fold change, FC) showed a significant upregulation of *SOCS3* (Wilcoxon rank sum test, $p \leq 0.05$), *ITGAL* (Wilcoxon rank sum test, $p \leq 0.05$), *NFIC* (Wilcoxon rank sum test, $p \leq 0.05$), *NCOR2* (Wilcoxon rank sum test, $p \leq 0.05$), and *PGK1* (Wilcoxon

rank sum test, $p \leq 0.05$) mRNA levels in PAH patients vs. CTRLs (Fig. 5). Since the network-oriented *SOCS3* gene is a negative feedback mediator of the IL-6 signaling [37–40], we investigated the transcriptional profiles of *IL-6*, IL-6 receptor (*IL-6R*), and signal transducer and activator of transcription 3 (*STAT3*) genes. The mRNA levels of the *IL-6* (Wilcoxon rank sum test, $p \leq 0.05$) and *STAT3* (Wilcoxon rank sum test, $p \leq 0.05$) genes were significantly upregulated in PAH patients vs. CTRLs. Among the transcriptional profiles evaluated in the PAH subnetwork, only the IL-6 upregulation significantly distinguished IPAH vs. Associated-PAH (Wilcoxon rank sum test, $p \leq 0.05$) (Fig. 5) suggesting a potential phenotype-specific biomarker or drug target.

Expression Profile of the Network-Oriented *SOCS3* Protein Discriminates PAH Patients vs. CTRLs

We further focused our attention on the network-oriented *SOCS3* gene for two reasons: first, *SOCS3* was the most recurrent gene among the top significant pathways into the PAH subnetwork (Fig. 3); second, *SOCS3* promoter hypomethylation was negatively associated with RAP and positively associated CI in both IPAH

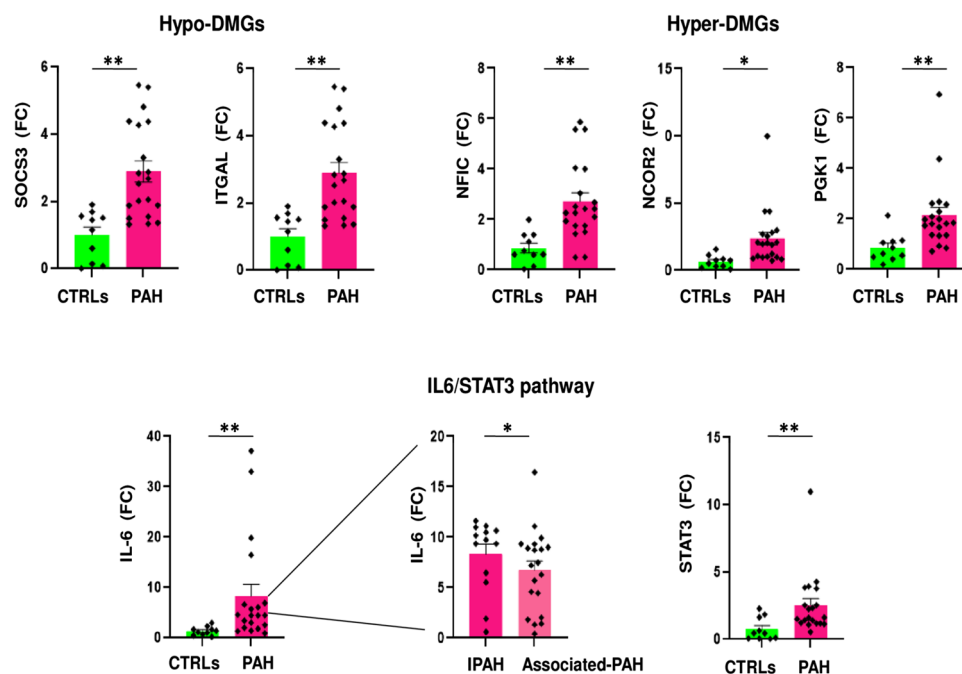


Fig. 5 Network-oriented transcriptional profiles. Dot plots show the relative expression (FC) of hypomethylated and hypermethylated network-oriented DMGs and IL-6/STAT3 signaling axis in PBMCs from $N=20$ PAH patients vs. $N=10$ CTRLs (Wilcoxon rank sum exact test, $*p < 0.05$ vs. controls; $**p < 0.01$ vs. controls). Dot plots were performed using GraphPad Prism version 9.0.0 software. Abbreviations: ITGAL integrin subunit alpha L; GNAS, guanine

nucleotide binding protein (G protein), alpha stimulating activity; GRM2, glutamate metabotropic receptor 2; LIMS2, LIM zinc finger domain containing 2; NCOR2, nuclear receptor corepressor 2; NFIC, nuclear factor I C; NR4A2, nuclear receptor subfamily 4 group A member 2; PAH, pulmonary arterial hypertension; PGK1, phosphoglycerate kinase 1; *SOCS3*, suppressor of cytokine signaling 3

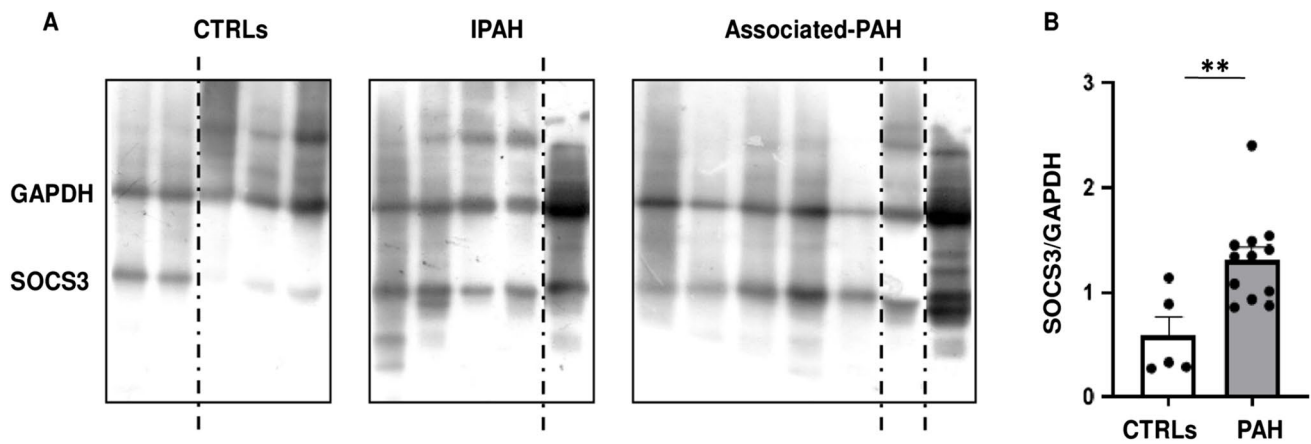


Fig. 6 Network-oriented *SOCS3* expression profile. **A** Western blot analysis of *SOCS3* protein expression in PBMCs isolated from CTRLs ($N=5$) vs. IPAH ($N=5$) and Associated-PAH ($N=7$). The dashed black lines correspond to the cuts in the original film. **B** The dot plot shows the absolute values of the *SOCS3*/GAPDH ratio for each study participant. *SOCS3* protein expression was significantly

higher in PAH patients vs. CTRLs (two-tailed t -test; $**p < 0.01$). Dot plot was performed using GraphPad Prism version 9.0.0 software. Abbreviations: CTRLs, controls; GAPDH, glyceraldehyde-3-phosphate dehydrogenase; IPAH, idiopathic pulmonary arterial hypertension; *SOCS3*, suppressor of cytokine signaling 3

and Associated-PAH patients suggesting a biomarker of poor hemodynamics (Fig. 4B–C). Based on the availability and quality of PBMCs, we measured the expression of the *SOCS3* protein by immunoblot in $N=5$ CTRLs vs. $N=5$ IPAH and $N=7$ Associated-PAH patients (Fig. 6A and Supplementary Fig. 9). Clinical characteristics of PAH patients are described in Supplementary Table 14. According to *SOCS3* promoter hypomethylation in $CD4^+$ T cells and upregulation of mRNA levels in PBMCs (Fig. 5), we found that *SOCS3* protein levels were significantly higher in PAH patients vs. CTRLs (Fig. 6B), with no difference between IPAH vs. Associated-PAH (two-tailed t -test; $p < 0.05$). This lets us to speculate that *SOCS3* might represent a hub gene in PAH pathogenesis and its progression.

Discussion

The major findings of the present study are as follows: (1) circulating $CD4^+$ T cell promoter methylation levels informed a network-based approach to identifying *SOCS3*, *GNAS*, *ITGAL*, *NCOR2*, *NFIC*, *NR4A2*, *GRM2*, *PGK1*, *STMN1*, and *LIMS2* genes as potentially involved in PAH pathogenesis or its progression, a finding that was validated by demonstrating that these genes strongly associated with RAP, CI, mPAP, or PVR; (2) mRNA levels of the network-oriented *SOCS3*, *ITGAL*, *NFIC*, *NCOR2*, and *PGK1* genes were significantly upregulated in PBMCs isolated from PAH patients vs. CTRLs; (3) of note, the *SOCS3* promoter hypomethylation correlated inversely with RAP and CI both in IPAH and Associated-PAH suggesting a potential prognostic

biomarker; and (4) a significant *SOCS3* gene overexpression was confirmed at protein level in PBMCs from PAH patients vs. CTRLs supporting its role as hub gene in PAH.

The goal of our study was to apply a novel network-oriented approach to patient-derived $CD4^+$ T cell methylation profiles in order to identify potential PAH candidate genes and molecular pathways able to mirror clinical information. Interestingly, both in IPAH and Associated-PAH, *SOCS3* hypomethylation was negatively correlated with RAP and positively correlated with CI which are the most robust parameters of right ventricle function and prognosis in PAH. Despite the fact that association does not mean causation, this let us hypothesize that DNA methylation changes of the *SOCS3* gene might have a role in disease onset and its progression. Also, previous evidence reported an upregulation of *SOCS3* mRNA levels in fibroblast-activated macrophages accumulated in pulmonary arterioles from IPAH patients and a parallel upregulation of IL-6/STAT3 axis suggesting a potential drug target [31].

Promoter hypomethylation of the *ITGAL* gene in $CD4^+$ T cells may contribute to its mRNA overexpression in PMBCs of patients with PAH vs. CTRLs. Also known as CD11a, the *ITGAL* gene encodes for the alpha L chain of integrins. The *ITGAL* protein is essential to inflammatory and immune responses by regulating adhesive and co-stimulatory interactions between $CD4^+$ T cells and other cells. No evidence exists for involvement of the *ITGAL* gene in PAH; however, a prior study reported a parallel hypomethylation and mRNA overexpression of the *ITGAL* gene in circulating $CD4^+$ T cells isolated from 18 patients with systemic sclerosis (of which only one had PAH) vs. 15 CTRLs leading to immunological abnormalities and fibrotic processes [41]. Thus,

upregulation of the *ITGAL* gene may guide transmigration of CD4⁺ T cells and consequent infiltration into small pulmonary arterioles exacerbating vascular remodeling in PAH.

Despite the fact that *PGK1*, *NFIC*, and *NCOR2* gene promoters were hypermethylated in specific CpG sites, we found significantly increased mRNA levels in PBMCs of patients with PAH vs. CTRLs. This observation is in line with prior evidence showing a positive correlation between DNA methylation and gene expression in certain systems, thus countering the traditional dogma [42]. An explanation for this finding may be that DNA methylation is not itself alone sufficient to define the spectrum of gene expression but may only affect genes that are already silenced by other epigenetic-sensitive mechanisms [43]. In fact, the specific location of the methylation and its interaction with other epigenetic factors, particularly histone modifications and DNA-binding transcription factors, provide additional complexity to DNA methylation-dependent gene regulation processes [5].

A major strength of our study was the use of CD4⁺ T cells purified from peripheral blood specimens collected during RHC at first diagnosis (> 70%) or early follow-up (within 1 year). While it is true that lung tissues are necessary to potentially link methylation signatures to PAH pathogenesis, a great limitation is that lung biopsy is not usually performed in the routine management of PAH. Consequently, lung tissues are available only from end-stage PAH patients undergoing lung transplantation who were largely enrolled in previous omics-based analyses [1]. It is very difficult to clarify whether DNA methylation changes in lung tissues are really PAH-specific because the epigenome of end-stage patients might be merely a consequence of the overall compromised pulmonary status rather than a mirror of early drivers of disease.

Our interest on CD4⁺ T cells first arose from the evidence that pulmonary lesions in PAH patients are sites of a marked infiltration of CD4⁺ T cells [13–16]. In addition, CD4⁺ T cells with protective roles (Tregs) migrated to the lung in the early stages of PAH to suppress pulmonary inflammation [11], whereas Th2 cells contributed to muscularization of the pulmonary arterioles [12]. Our focus on circulating CD4⁺ T cells was particularly strengthened by prior data showing that the bone morphogenetic protein receptor type 2 (*BMPR2*) signaling axis, as a major driver of PAH pathogenesis [1], may contribute to thymic homeostasis by regulating commitment and differentiation of the T cell lineage [44]. Taken together, we considered reasonable and attractive the use of circulating CD4⁺ T cells to evaluate whether DNA methylation changes associated with hemodynamics, potentially informing the identification of readily accessible prognostic biomarkers.

Globally, our RRBS and subsequent network-oriented analysis showed that circulating CD4⁺ T cells were

preferentially hypermethylated in PAH patients vs. CTRLs. This finding may be consistent with deleterious loss-of-function mutations in the ten-eleven translocation (TET) 2 demethylating enzyme found in Caucasian patients with IPAH associated with increased inflammation [6]. Previous studies suggested that promoter hypermethylation both in PBMCs and lung tissues was associated with *BMPR2* gene downregulation and progression of PAH [45, 46]. Interestingly, Bissierier et al. [46] demonstrated that an increased expression of the SIN3 transcription regulator family member A (SIN3A) repressor downregulated the levels of DNA methyltransferase 1 (DNMT1) while promoting the expression of the DNA demethylase TET1 in human pulmonary artery smooth muscle cells suggesting a potential epigenetic-based approach to attenuate PAH. Compared to previous studies, our genome-wide differential DNA methylation analysis did not identify specific dmCpGs annotated to the *BMPR2* promoter gene. The underlying reason can be that DNA methylation signatures are strongly dependent on cellular type as well as they can vary on the basis of sequencing platforms. We chose RRBS for the discovery analysis for two reasons: first, it is a preferable quantitative assay for revealing unusual methylated loci and minimizing DNA loss due to bisulfite-induced degradation when sample quantity is limited [47]; second, RRBS provides an enrichment in CGIs and promoter regions. We next performed the Infinium Human Methylation EPIC BeadChip analysis which employs oligonucleotide hybridization probes targeting CpG sites of interest in the validation cohort. Of note, the methylation trend for the network-oriented DMGs of the PAH subnetwork was the same in both next-generation sequencing platforms.

Our study presents some limitations. First, this is a pilot study aimed at exploring a novel research strategy which integrates DNA methylation, network analysis, and hemodynamics in PAH patients. The small size of both discovery and validation sets as well as their clinical heterogeneity do not allow to get a secure finding. Besides, the intrinsic nature of the epigenome-wide association studies do not allow to infer a cause-effect relationship of our PAH network-oriented candidate genes. Since diagnosis of PAH generally occurs in older patients, it was impossible to match PAH patients and blood donor volunteers for age, as described in another study [48]. However, no statistical difference in distribution of age for both CTRLs and PAH patients was found (Wilcoxon rank sum test, $p = 0.07$) (Data Supplement). Additionally, a linear regression analysis between the DNA methylation levels of each network-oriented DMGs and the age of both CTRLs and PAH patients revealed that the predictor variable (age) was not significantly related to the outcome variable (DMGs) for 8/10 network-oriented genes (Supplementary Fig. 10). According to a previous study [49], we can rule out the possibility that differential DNA methylation signatures between CTRLs and PAH

patients may be due to the age. Furthermore, due to availability of biological biospecimens from our study population, we were not able to perform experimental validation (qRT-PCR and Western Blot) on CD4⁺ T cells but only in PBMC fraction. Larger prospective studies are needed to evaluate whether network-oriented DMGs may be used as potential biomarkers to optimize prognosis in PAH [1, 3, 50–52]. Nonetheless, circulating DNA methylome analyzed via network analysis may yield insight into early disease pathogenesis and suggest noninvasive biomarkers that can be used to optimize patient phenotyping and, possibly, predicted outcome in PAH.

Supplementary Information The online version contains supplementary material available at <https://doi.org/10.1007/s12265-022-10294-1>.

Acknowledgements The authors wish to thank Stephanie Tribuna for expert technical assistance; the authors thank the microarray unit of the DKFZ Genomics and Proteomics Core Facility for providing the Illumina Methylation Beadchips and related services. Dr. Giuditta Benincasa was supported during her PhD program by Educational Grant from the University of Campania “L. Vanvitelli”, Naples, Italy.

Author Contribution CN and GB conceptualized the study. GB designed the network analysis strategy. OA and MF performed the bioinformatics analysis. GB, OA, and MF interpreted the data, drafted the manuscript, and designed illustrations used in the current work. CS and PB provided technical experimental support. MDA, PA, ER, and PG coordinated the enrollment of patients and supported this study with their expertise in management of pulmonary arterial hypertension. BAM, LB, JL, and CN critically revised the manuscript for important intellectual content.

Funding Open access funding provided by Università degli Studi della Campania Luigi Vanvitelli within the CRUI-CARE Agreement. This work was supported by PRIN2017F8ZB89 from “Italian Ministry of University and Research (MIUR)” (PI Prof Napoli) and Ricerca Corrente (RC) 2019 from “Italian Ministry of Health” (PI Prof. Napoli).

Data Availability All raw data obtained from RRBS and Infinium Human Methylation EPIC BeadChip platforms have been uploaded to the NCBI GEO database (accession ID: GSE165360).

Declarations

Competing Interests The authors declare no competing interests.

Open Access This article is licensed under a Creative Commons Attribution 4.0 International License, which permits use, sharing, adaptation, distribution and reproduction in any medium or format, as long as you give appropriate credit to the original author(s) and the source, provide a link to the Creative Commons licence, and indicate if changes were made. The images or other third party material in this article are included in the article's Creative Commons licence, unless indicated otherwise in a credit line to the material. If material is not included in the article's Creative Commons licence and your intended use is not permitted by statutory regulation or exceeds the permitted use, you will need to obtain permission directly from the copyright holder. To view a copy of this licence, visit <http://creativecommons.org/licenses/by/4.0/>.

References

- Napoli C, Benincasa G, Loscalzo J. Epigenetic inheritance underlying pulmonary arterial hypertension. *Arterioscler Thromb Vasc Biol.* 2019;39:653–64. <https://doi.org/10.1161/ATVBAHA.118.312262>.
- Farber HW, Loscalzo J. Pulmonary arterial hypertension. *N Engl J Med.* 2004;351:1655–65. <https://doi.org/10.1056/NEJMra035488>.
- Benincasa G, DeMeo DL, Glass K, Silverman EK, Napoli C. Epigenetics and pulmonary diseases in the horizon of precision medicine: a review. *Eur Respir J.* 2021;57:2003406. <https://doi.org/10.1183/13993003.03406-2020>.
- D'Alto M, Badagliacca R, Argiento P, Romeo E, Farro A, Papa S, Sarubbi B, Russo MG, Vizza CD, Golino P, Naeije R. Risk reduction and right heart reverse remodeling by upfront triple combination therapy in pulmonary arterial hypertension. *Chest.* 2020;157:376–83. <https://doi.org/10.1016/j.chest.2019.09.009>.
- Jones PA. Functions of DNA methylation: islands, start sites, gene bodies and beyond. *Nat Rev Genet.* 2012;13:484–92. <https://doi.org/10.1038/nrg3230>.
- Potus F, Pauciulo MW, Cook EK, Zhu N, Hsieh A, Welch CL, Shen Y, Tian L, Lima P, Mewburn J, D'Arsigny CL, Lutz KA, Coleman AW, Damico R, Snetsinger B, Martin AY, Hassoun PM, Nichols WC, Chung WK, Rauh MJ, Archer SL. Novel mutations and decreased expression of the epigenetic regulator TET2 in pulmonary arterial hypertension. *Circulation.* 2020;16(141):1986–2000. <https://doi.org/10.1161/CIRCULATIONAHA.119.044320>.
- Rabinovitch M, Guignabert C, Humbert M, Nicolls MR. Inflammation and immunity in the pathogenesis of pulmonary arterial hypertension. *Circ Res.* 2014;115:165–75. <https://doi.org/10.1161/CIRCRESAHA.113.301141>.
- Voelkel NF, Tamosiuniene R, Nicolls MR. Challenges and opportunities in treating inflammation associated with pulmonary hypertension. *Expert Rev Cardiovasc Ther.* 2016;14:939–51. <https://doi.org/10.1080/14779072.2016.1180976>.
- Taraseviciene-Stewart L, Nicolls MR, Kraskauskas D, Scerbavicius R, Burns N, Cool C, Wood K, Parr JE, Boackle SA, Voelkel NF. Absence of T cells confers increased pulmonary arterial hypertension and vascular remodeling. *Am J Respir Crit Care Med.* 2007;175:1280–9. <https://doi.org/10.1164/rccm.200608-1189OC>.
- Miyata M, Sakuma F, Ito M, Ohira H, Sato Y, Kasukawa R. Athymic nude rats develop severe pulmonary hypertension following monocrotaline administration. *Int Arch Allergy Immunol.* 2000;121:246–52. <https://doi.org/10.1159/000024324>.
- Tamosiuniene R, Tian W, Dhillon G, Wang L, Sung YK, Gera L, Patterson AJ, Agrawal R, Rabinovitch M, Ambler K, Long CS, Voelkel NF, Nicolls MR. Regulatory T cells limit vascular endothelial injury and prevent pulmonary hypertension. *Circ Res.* 2011;109:867–9. <https://doi.org/10.1161/CIRCRESAHA.110.236927>.
- Daley E, Emson C, Guignabert C, de Waal MR, Louten J, Kurup VP, Hogaboam C, Taraseviciene-Stewart L, Voelkel NF, Rabinovitch M, Grunig E, Grunig G. Pulmonary arterial remodeling induced by a Th2 immune response. *J Exp Med.* 2008;205:361–72. <https://doi.org/10.1084/jem.20071008>.
- Savai R, Pullamsetti SS, Kolbe J, Bieniek E, Voswinckel R, Fink L, Scheed A, Ritter C, Dahal BK, Vater A, Klussmann S, Ghofrani HA, Weissmann N, Klepetko W, Banat GA, Seeger W, Grimminger F, Schermuly RT. Immune and inflammatory cell involvement in the pathology of idiopathic pulmonary arterial hypertension. *Am J Respir Crit Care Med.* 2012;186:897–908. <https://doi.org/10.1164/rccm.201202-0335OC>.

14. Marsh LM, Jandl K, Grünig G, Foris V, Bashir M, Ghanim B, Klepetko W, Olschewski H, Olschewski A, Kwapiszewska G. The inflammatory cell landscape in the lungs of patients with idiopathic pulmonary arterial hypertension. *Eur Respir J*. 2018;51:1701214. <https://doi.org/10.1183/13993003.01214-2017>.
15. Hautefort A, Girerd B, Montani D, Cohen-Kaminsky S, Price L, Lambrecht BN, Humbert M, Perros F. T-helper 17 cell polarization in pulmonary arterial hypertension. *Chest*. 2015;147:1610–20. <https://doi.org/10.1378/chest.14-1678>.
16. Cuttica MJ, Langenickel T, Noguchi A, Machado RF, Gladwin MT, Boehm M. Perivascular T-cell infiltration leads to sustained pulmonary artery remodeling after endothelial cell damage. *Am J Respir Cell Mol Biol*. 2011;45:62–71. <https://doi.org/10.1165/rcmb.2009-0365OC>.
17. Benincasa G, Franzese M, Schiano C, Marfella R, Miceli M, Infante T, Sardu C, Zanfardino M, Affinito O, Mansueto G, Sommese L, Nicoletti GF, Salvatore M, Paolisso G, Napoli C. DNA methylation profiling of CD4+/CD08+ T cells reveals pathogenic mechanisms in increasing hyperglycemia: PIRAMIDE pilot study. *Ann Med Surg (Lond)*. 2020;60:218–26. <https://doi.org/10.1016/j.amsu.2020.10.016>.
18. Infante T, Franzese M, Ruocco A, Schiano C, Affinito O, Pane K, Memoli D, Rizzo F, Weisz A, Bontempo P, Grimaldi V, Berrino L, Soricelli A, Mauro C, Napoli C. ABCA1, TCF7, NFATC1, PRKCZ, and PDGFA DNA methylation as potential epigenetic-sensitive targets in acute coronary syndrome via network analysis. *Epigenetics*. 2021;17:547–63. <https://doi.org/10.1080/15592294.2021.1939481>.
19. Galiè N, Humbert M, Vachiery JL, Gibbs S, Lang I, Torbicki A, Simonneau G, Peacock A, Vonk Noordegraaf A, Beghetti M, Ghofrani A, Gomez Sanchez MA, Hansmann G, Klepetko W, Lancellotti P, Matucci M, McDonagh T, Pierard LA, Trindade PT, Zompatori M, Hoeper M. 2015 ESC/ERS Guidelines for the diagnosis and treatment of pulmonary hypertension. *Rev Esp Cardiol (Engl Ed)*. 2016;69:177. <https://doi.org/10.1016/j.rec.2016.01.002>.
20. Rienzo M, Schiano C, Casamassimi A, Grimaldi V, Infante T, Napoli C. Identification of valid reference housekeeping genes for gene expression analysis in tumor neovascularization studies. *Clin Transl Oncol*. 2013;15:211–8. <https://doi.org/10.1007/s12094-012-0904-1>.
21. Akalin A, Kormaksson M, Li S, Garrett-Bakelman FE, Figueroa ME, Melnick A, Mason CE. MethyKit: a comprehensive R package for the analysis of genome-wide DNA methylation profiles. *Genome Biol*. 2012;13:87. <https://doi.org/10.1186/gb-2012-13-10-r87>.
22. Yu G, Wang LG, He QY. ChIPseeker: an R/Bioconductor package for ChIP peak annotation, comparison and visualization. *Bioinformatics*. 2015;31:2382–3. <https://doi.org/10.1093/bioinformatics/btv145>.
23. Zhou G, Soufan O, Ewald J, Hancock REW, Basu N, Xia J. NetworkAnalyst 3.0: a visual analytics platform for comprehensive gene expression profiling and meta-analysis. *Nucleic Acids Res*. 2019;47:234–41. <https://doi.org/10.1093/nar/gkz240>.
24. Piñero J, Ramírez-Anguaita JM, Saüch-Pitarch J, Ronzano F, Centeno E, Sanz F, Furlong LL. The DisGeNET knowledge platform for disease genomics: 2019 update. *Nucleic Acids Res*. 2020;48:845–55. <https://doi.org/10.1093/nar/gkz1021>.
25. Shannon P, Markiel A, Ozier O, Baliga NS, Wang JT, Ramage D, Amin N, Schwikowski B, Ideker T. Cytoscape: a software environment for integrated models of biomolecular interaction networks. *Genome Res*. 2003;13:2498–504. <https://doi.org/10.1101/gr.1239303>.
26. Wu G, Dawson E, Duong A, Haw R, Stein L (2014) Reactome-FIViz: a Cytoscape app for pathway and network-based data analysis. Version 2. F1000Res 3:146. <https://doi.org/10.12688/f1000research.4431.2>.
27. Doncheva NT, Assenov Y, Domingues FS, Albrecht M. Topological analysis and interactive visualization of biological networks and protein structures. *Nat Protoc*. 2012;7:670–85. <https://doi.org/10.1038/nprot.2012.004>.
28. Aghamohammadzadeh R, Zhang YY, Stephens TE, Arons E, Zaman P, Polach KJ, Matar M, Yung LM, Yu PB, Bowman FP, Opatowsky AR, Waxman AB, Loscalzo J, Leopold JA, Maron BA. Up-regulation of the mammalian target of rapamycin complex 1 subunit Raptor by aldosterone induces abnormal pulmonary artery smooth muscle cell survival patterns to promote pulmonary arterial hypertension. *FASEB J*. 2016;30:2511–27. <https://doi.org/10.1096/fj.201500042>.
29. Hemnes AR, Zhao M, West J, Newman JH, Rich S, Archer SL, Robbins IM, Blackwell TS, Cogan J, Loyd JE, Zhao Z, Gaskill C, Jetter C, Kropski JA, Majka SM, Austin ED. Critical genomic networks and vasoreactive variants in idiopathic pulmonary arterial hypertension. *Am J Respir Crit Care Med*. 2016;194:464–75. <https://doi.org/10.1164/rccm.201508-1678OC>.
30. Holda MK, Stachowicz A, Suski M, Wojtysiak D, Sowińska N, Arent Z, Palka N, Podolec P, Kopeć G. Myocardial proteomic profile in pulmonary arterial hypertension. *Sci Rep*. 2020;10:14351. <https://doi.org/10.1038/s41598-020-71264-8>.
31. El Kasmī KC, Pugliese SC, Riddle SR, Poth JM, Anderson AL, Frid MG, Li M, Pullamsetti SS, Savai R, Nagel MA, Fini MA, Graham BB, Tudor RM, Friedman JE, Eltzschig HK, Sokol RJ, Stenmark KR. Adventitial fibroblasts induce a distinct proinflammatory/profibrotic macrophage phenotype in pulmonary hypertension. *J Immunol*. 2014;193:597–609. <https://doi.org/10.4049/jimmunol.1303048>.
32. Satoh K, Satoh T, Kikuchi N, Omura J, Kurosawa R, Suzuki K, Sugimura K, Aoki T, Nochioka K, Tatebe S, Miyamichi-Yamamoto S, Miura M, Shimizu T, Ikeda S, Yaoita N, Fukumoto Y, Minami T, Miyata S, Nakamura K, Ito H, Kadomatsu K, Shimokawa H. Basigin mediates pulmonary hypertension by promoting inflammation and vascular smooth muscle cell proliferation. *Circ Res*. 2014;115:738–50. <https://doi.org/10.1161/CIRCRESAHA.115.304563>.
33. Schimmel L, van der Stoel M, Rianna C, van Stalborch AM, de Ligt A, Hoogenboezem M, Tol S, van Rijssel J, Szulcek R, Bogaard HJ, Hofmann P, Boon R, Radmacher M, de Waard V, Huvneers S, van Buul JD. Stiffness-induced endothelial DLC-1 expression forces leukocyte spreading through stabilization of the ICAM-1 adhesome. *Cell Rep*. 2018;24:3115–24. <https://doi.org/10.1016/j.celrep.2018.08.045>.
34. Benza RL, Gomberg-Maitland M, Demarco T, Frost AE, Torbicki A, Langleben D, Pulido T, Correa-Jaque P, Passineau MJ, Wiener HW, Tamari M, Hirota T, Kubo M, Tiwari HK. Endothelin-1 pathway polymorphisms and outcomes in pulmonary arterial hypertension. *Am J Respir Crit Care Med*. 2015;192:1345–54. <https://doi.org/10.1164/rccm.201501-0196OC>.
35. Silverman EK, Schmidt HHHW, Anastasiadou E, Altucci L, Angelini M, Badimon L, Balligand JL, Benincasa G, Capasso G, Conte F, Di Costanzo A, Farina L, Fison G, Gatto L, Gentili M, Loscalzo J, Marchese C, Napoli C, Paci P, Petti M, Quackenbush J, Tieri P, Viggiano D, Vilahur G, Glass K, Baumbach J (2020) Molecular networks in network medicine: development and applications. *Wiley Interdiscip Rev Syst Biol Med* e1489. <https://doi.org/10.1002/wsbm.1489>.
36. Benincasa G, Marfella R, Della Mura N, Schiano C, Napoli C. Strengths and opportunities of network medicine in cardiovascular diseases. *Circ J*. 2020;84:144–52. <https://doi.org/10.1253/circj.CJ-19-0879>.
37. Paulin R, Courboulin A, Meloche J, Mainguy V, Dumas de la Roque E, Saksouk N, Côté J, Provencher S, Sussman MA, Bonnet

- S. Signal transducers and activators of transcription-3/pim1 axis plays a critical role in the pathogenesis of human pulmonary arterial hypertension. *Circulation*. 2011;123:1205–15. <https://doi.org/10.1161/CIRCULATIONAHA.110.963314>.
38. Brock M, Trenkmann M, Gay RE, Michel BA, Gay S, Fischler M, Ulrich S, Speich R, Huber LC. Interleukin-6 modulates the expression of the bone morphogenic protein receptor type II through a novel STAT3-microRNA cluster 17/92 pathway. *Circ Res*. 2009;104:1184–91. <https://doi.org/10.1161/CIRCRESAHA.109.197491>.
 39. Hashimoto-Kataoka T, Hosen N, Sonobe T, Arita Y, Yasui T, Masaki T, Minami M, Inagaki T, Miyagawa S, Sawa Y, Murakami M, Kumanogoh A, Yamauchi-Takahara K, Okumura M, Kishimoto T, Komuro I, Shirai M, Sakata Y, Nakaoka Y. Interleukin-6/interleukin-21 signaling axis is critical in the pathogenesis of pulmonary arterial hypertension. *Proc Natl Acad Sci U S A*. 2015;112:2677–86. <https://doi.org/10.1073/pnas.1424774112>.
 40. Xiang S, Dong NG, Liu JP, Wang Y, Shi JW, Wei ZJ, Hu XJ, Gong L. Inhibitory effects of suppressor of cytokine signaling 3 on inflammatory cytokine expression and migration and proliferation of IL-6/IFN- γ -induced vascular smooth muscle cells. *J Huazhong Univ Sci Technolog Med Sci*. 2013;33:615–22. <https://doi.org/10.1007/s11596-013-1168-x>.
 41. Wang Y, Shu Y, Xiao Y, Wang Q, Kanekura T, Li Y, Wang J, Zhao M, Lu Q, Xiao R. Hypomethylation and overexpression of ITGAL (CD11a) in CD4(+) T cells in systemic sclerosis. *Clin Epigenetics*. 2014;6:25. <https://doi.org/10.1186/1868-7083-6-25>.
 42. Anastasiadi D, Esteve-Codina A, Piferrer F. Consistent inverse correlation between DNA methylation of the first intron and gene expression across tissues and species. *Epigenetics Chromatin*. 2018;11:37. <https://doi.org/10.1186/s13072-018-0205-1>.
 43. Bird A. DNA methylation patterns and epigenetic memory. *Genes Dev*. 2002;16:6–21. <https://doi.org/10.1101/gad.947102>.
 44. Hager-Theodorides AL, Outram SV, Shah DK, Sacedon R, Shrimpton RE, Vicente A, Varas A, Crompton T. Bone morphogenetic protein 2/4 signaling regulates early thymocyte differentiation. *J Immunol*. 2002;169:5496–504. <https://doi.org/10.4049/jimmunol.169.10.5496>.
 45. Liu D, Yan Y, Chen JW, Yuan P, Wang XJ, Jiang R, Wang L, Zhao QH, Wu WH, Simonneau G, Qu JM, Jing ZC. Hypermethylation of BMPR2 promoter occurs in patients with heritable pulmonary arterial hypertension and inhibits BMPR2 expression. *Am J Respir Crit Care Med*. 2017;196:925–8. <https://doi.org/10.1164/rccm.201611-2273LE>.
 46. Bissierier M, Mathiyalagan P, Zhang S, Elmastour F, Dorfmueller P, Humbert M, David G, Tarzami S, Weber T, Perros F, Sassi Y, Sahoo S, Hadri L. Regulation of the methylation and expression levels of the BMPR2 gene by SIN3a as a novel therapeutic mechanism in pulmonary arterial hypertension. *Circulation*. 2021;144:52–73. <https://doi.org/10.1161/CIRCULATIONAHA.120.047978>.
 47. Walker DL, Bhagwate AV, Baheti S, Smalley RL, Hilker CA, Sun Z, Cunningham JM. DNA methylation profiling: comparison of genome-wide sequencing methods and the Infinium Human Methylation 450 Bead Chip. *Epigenomics*. 2015;7:1287–302. <https://doi.org/10.2217/EPI.15.64>.
 48. Jones MJ, Goodman SJ, Kobor MS. DNA methylation and healthy human aging. *Aging Cell*. 2015;14:924–32. <https://doi.org/10.1111/ace1.12349>.
 49. Hautefort A, Chesné J, Preussner J, Pullamsetti SS, Tost J, Looso M, Antigny F, Girerd B, Riou M, Eddahibi S, Deleuze JF, Seeger W, Fadel E, Simonneau G, Montani D, Humbert M, Perros F. Pulmonary endothelial cell DNA methylation signature in pulmonary arterial hypertension. *Oncotarget*. 2017;8:52995–3016. <https://doi.org/10.18632/oncotarget.18031>.
 50. Wang RS, Loscalzo J. Network module-based drug repositioning for pulmonary arterial hypertension. *CPT Pharmacometrics Syst Pharmacol*. 2021;10:994–1005. <https://doi.org/10.1002/psp4.12670>.
 51. Sarno F, Benincasa G, List M, Barabasi AL, Baumbach J, Ciardiello F, Filetti S, Glass K, Loscalzo J, Marchese C, Maron BA, Paci P, Parini P, Petrillo E, Silverman EK, Verrienti A, Altucci L, Napoli C, International Network Medicine Consortium. Clinical epigenetics settings for cancer and cardiovascular diseases real-life applications of network medicine at the bedside. *Clin Epigenetics*. 2021;13:66. <https://doi.org/10.1186/s13148-021-01047-z>.
 52. Napoli C, Loscalzo J. Nitric oxide and other novel therapies for pulmonary hypertension. *J Cardiovasc Pharmacol Ther*. 2004;9(1):1–8. <https://doi.org/10.1177/107424840400900i101>.

Publisher's Note Springer Nature remains neutral with regard to jurisdictional claims in published maps and institutional affiliations.